Scripta Materialia 182 (2020) 53–56

Contents lists available at ScienceDirect

Scripta Materialia

journal homepage: www.elsevier.com/locate/scriptamat

The effect of solute cloud formation on the second order pyramidal to basal transition of $\langle \mathbf{c}+\mathbf{a} \rangle$ edge dislocations in Mg-Y solid solutions

Daniel Utt[a,b], Alexander Stukowski[a], Maryam Ghazisaeidi[b,*]

[a] Fachgebiet Materialmodellierung, Institut für Materialwissenschaft, TU Darmstadt, Otto-Berndt-Str. 3, Darmstadt D-64287, Germany
[b] Materials Science and Engineering, Ohio State University, 2041 College Rd, Columbus, OH 43210, USA

ARTICLE INFO

Article history:
Received 1 October 2019
Revised 17 February 2020
Accepted 19 February 2020
Available online 6 March 2020

Keywords:
Mg-Y alloys
$\langle c+a \rangle$ slip
Segregation
Monte Carlo
Molecular dynamics

ABSTRACT

We study the effect of solute segregation on pyramidal to basal transformation of $\langle c+a \rangle$ edge dislocations in a model Mg-Y alloy, using a hybrid Monte Carlo/Molecular Dynamics method. While a random solute distribution has no appreciable effect on this undesirable transition, a solute cloud around the dislocation slows and effectively prevents it in case of Mg-3 at % Y alloy. Comparing with the time scale required for diffusion of Y to the dislocation, suggests that segregation of Y and other fast diffusing elements can be engineered to prohibit this glissile to sessile transition, and stabilize the pyramidal glide of $\langle c+a \rangle$ dislocations.

© 2020 Acta Materialia Inc. Published by Elsevier Ltd. All rights reserved.

Magnesium (Mg) is a light metal– 4.6 times lighter than conventional steels and 1.6 times lighter than aluminum (Al) [1] – making it suitable for use in automotive and aerospace applications in an effort to reduce weight and thereby enhancing fuel efficiency [2–11]. However, Mg has a naturally low ductility and fracture toughness reducing its viability for structural applications.

The reduced ductility in Mg is caused by the fact that plastic deformation in the $\langle \mathbf{c} \rangle$ direction is carried by glissle $\langle \mathbf{c}+\mathbf{a} \rangle$ dislocations on the pyramidal (py) II planes [12]. Even at room temperature pyII $\langle \mathbf{c}+\mathbf{a} \rangle$ dislocations spontaneously transition into the energetically more favorable basal $\langle \mathbf{c}+\mathbf{a} \rangle$ dislocations [13]. These newly formed dislocations in the basal plane are sessile and cannot contribute to plastic flow at reasonable applied stresses. Delaying or preventing the pyII to basal transition (PBT) is therefore crucial to retaining the ductility of Mg.

Experimental studies have shown an increase in the ductility of the Mg-Y alloys, which is thought to be due to increased activity of pyII $\langle \mathbf{c}+\mathbf{a} \rangle$ dislocations [14–17]. This increase was initially attributed to favorable solute-I_1 stacking fault interactions [16,18]; a theory which was later questioned [19]. Another theory suggests, that the ductility enhancement from solute addition is caused by an increase in pyII to pyI cross-slip of $\langle \mathbf{c}+\mathbf{a} \rangle$ screw dislocations as a competing process counteracting the effects of PBT [20]. Moreover, it was recently shown that there is no effect on the characteristic PBT time in a random Mg-Y solid solution [21] compared to pure Mg samples [13].

The contrast between the findings of Ref. [21], showing unaffected PBT times in the Mg-Y, and experimental results showing strongly increased pyII dislocation activity in similar samples justifies further investigation of $\langle \mathbf{c}+\mathbf{a} \rangle$ dislocations in Mg-Y alloys. We used a similar methodology to the one used in Ref. [21], but instead of considering a *random* Mg-Y solid solution, we consider the possibility of solute segregation to the dislocations. We obtain the thermodynamic equilibrium solute concentration around the dislocation core via a Metropolis Monte-Carlo (MC) algorithm and show that pyII $\langle \mathbf{c}+\mathbf{a} \rangle$ dislocations can be stabilized as a result of solute accumulation in the strain field of the dislocation.

Atomistic simulations are performed with LAMMPS [22] using a Mg-Y modified embedded-atom method (MEAM) interatomic potential [23]. The simulation cell dimensions are 31 nm × 2.3 nm × 32 nm along x:$[2\bar{1}\bar{1}3]$, y:$[0\bar{1}10]$ and z: $[2\bar{1}\bar{1}\bar{2}]$: direction respectively. The dislocation line extends along the periodic y-direction. The other two boundaries have open surfaces. Atoms closer than 1.25 nm to the surface were fixed for all simulation. Three Mg-Y alloys are considered with Y concentrations of 0.33;1;3 *at.%*. At each composition, we created 300 different random configurations and selected the lowest energy ones for further studies. This accounts for the fact that dislocations in solid solutions tend to move to a local solute configuration with lower energy. Each cell was slightly rescaled based on the temperature dependent lattice constant of each composition.

* Corresponding author.
E-mail address: ghazisaeidi.1@osu.edu (M. Ghazisaeidi).

https://doi.org/10.1016/j.scriptamat.2020.02.033
1359-6462/© 2020 Acta Materialia Inc. Published by Elsevier Ltd. All rights reserved.

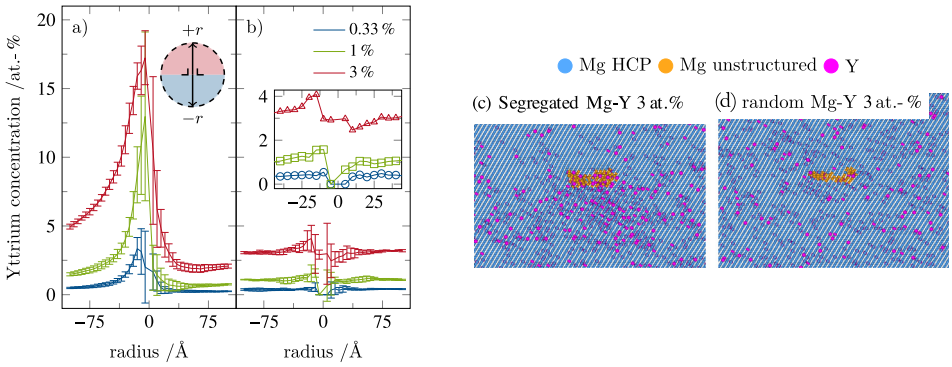

Fig. 1. Averaged radial Yttrium concentration profile and atomic arrangement in for the MgY_x samples. The average radial Y concentration of MC annealed samples is shown in (a) and those of the samples with a random atomic configuration in (b). Positive radii map to the compressive strain region of the dislocation, while negative radii extend into the tensile region (*cf.* the inset in (a), where the concentration is calculated for the respective shaded region). The inset in (b) shows a magnification around the dislocation core. Atomic arrangement close to the $\langle \mathbf{c}+\mathbf{a} \rangle$ pyII dislocation core in the MC equilibrated Mg-Y sample (c) and its random counterpart (d). The Mg atoms are color coded based on their local structure type [25]; hexagonal closest packing (HCP): blue, unstructured: yellow. All Y atoms are colored magenta. (For interpretation of the references to colour in this figure legend, the reader is referred to the web version of this article.)

The $\langle \mathbf{c}+\mathbf{a} \rangle$ dislocation is inserted on the pyII plane, assuming isotropic elasticity [12] using ATOMSK [24] and periodic boundary conditions along the dislocation line of 2.3 nm length. Atoms closer than 1.25 nm to the free surfaces are fixed during annealing and excluded from the MC trial moves. We compare three types of atomic arrangements: pure Mg, random Mg-Y solid solutions (random Mg-Y), and chemically equilibrated samples using a hybrid Monte Carlo/Molecular dynamics (MC/MD) method (MC Mg-Y). For each MC operation an atom swap in the canonical ensemble is attempted on 10 % of the atoms. These MC swaps were performed every 50 MD steps. We used a Nose-Hover thermostat during the MD steps.

The MC Mg-Y samples were chemically equilibrated for up to 40 ps using alternating MC and MD steps. Once the atomic configuration converge we proceed with only MD.

All samples were annealed at 700 $^\circ K$ using MD for up to 5 ns or until the PBT occurs. We found the transition time from sequential snapshots post-processed [25] and visualized in OVITO [26].

First, we quantify the excess Y concentration around the dislocation core in the random and the MC equilibrated samples and compare with the random Mg-Y results of Ref [21]. These concentrations are shown in Fig. 1. Here, we average the Y concentration around the initial $\langle \mathbf{c}+\mathbf{a} \rangle$ dislocation in concentric semi circles extending outwards. Positive radii go into the compressive region of the dislocation strain field, while negative radii cover the tensile side (*cf.* inset Fig. 1(a)). The concentration profiles are averaged over 8 samples.

Fig. 1(a) shows the Y concentration in the MC equilibrated samples. We can see that independent of the nominal bulk concentration a significant enrichment of Y in the tensile region of the dislocation strain field. This is the expected due the positive misfit volume [27] of Y in a Mg host lattice [23]. Similarly, the Y concentrations is reduced in the compressive region around the dislocation. Notably, all samples show Y concentrations higher than the solubility limit at 700 $^\circ K$ of $\approx$ 3 at. % [28] in the vicinity of the dislocation. The concentration profiles in the random Mg-Y sample (Fig. 1(b)) shows similar trend, albeit with much smaller concentration fluctuations around the dislocation core. The inset in (b) shows the region close to the core in more detail. These small deviations from the bulk concentration in the random sample can be explained by the fact that we selected energetically favorable random fluctuations around the dislocation during the initialization stage.

Fig. 1(c) and (d) shows two snapshots of the dislocation –after quenching to 0 $^\circ K$– in the $x_Y = 3$ at. % alloy after MC equilibration and in the random configuration respectively. Comparing the two structures, one can see that the MC steps lead to a Y enrichment, in the core of the dislocation in addition to the tensile region of its strain field. To further quantify these changes, we compare the radial pair distribution function (PDF) for the MC annealed sample and its random counterpart (Fig. 2(a,b)). Comparison of these PDFs, before and after MC annealing, shows a strong decrease in the nearest neighbor Y-Y bond count. Simultaneously, the Y-Y bond count at a distance of 5.7 Åincreases.

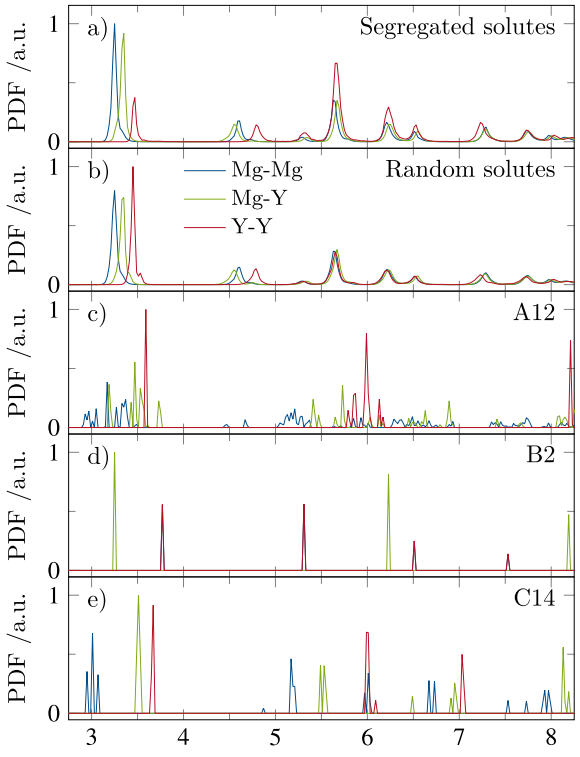

Fig. 2. Radial pair distribution function (PDF) for the segregated Mg-Y (a) and the random Mg-Y samples (b). Here we compare samples containing 3 at. % Y. For the MC sample we averaged 12 different atomic configurations, for the random one we averaged all 300 initially created arrangements. For comparison, the PDF of the three ordered intermetallic phases in the Mg-Y system are shown (c-e). For the C14 phase with partial occupancy 200 different arrangements were averaged. Note, that for the B2 phase Mg-Mg and Y-Y PDF peaks overlap. All PDFs are normalized between to 1.

Next, we analyze the possibility of new phase formation at the dislocation core by comparing the PDF with those of three ordered Mg-Y intermetallic phases: $Mg_{24}Y_5$ (A12), MgY (B2), and Mg_2Y (C14). The respective PDF fingerprint of each phase is given in Fig. 2(c–e). While the increase in Y-Y bond counts around 5.7 Åcould indicate the formation of A12 or C14 phase, both would also lead to an increase in Y-Y bond counts in the first nearest-neighbor shell. Since, we do not observe such an increase, the formation of an intermetallic phase seems unlikely. The reduction of Y-Y bonds in the nearest neighbor shell and the increase of Y-Y bond counts in a distance of 5.7 Å, can instead be attributed to the solute-solute interaction energy, predicted by this MEAM potential, as shown in Ref. [23]. While DFT predicts the second neighbor solute interactions to be strongly attractive, MEAM potential predicts this interaction to be moderately repulsive. Therefore, the trends observed in the PDF of the segregated dislocation, can be an artifact of the use of this MEAM potential.

Next, the simulation cells introduced in the previous section are annealed for up to 5 ns at 700°*K*to measure the PBT time. Said time as function of Y concentration and annealing procedure is given in Fig. 3(a) with reference data taken from Refs. [13,21] corresponding to pure Mg and random Mg-Y alloys respectively. The dashed horizontal line indicates the total annealing time. The PBT was not observed in all cases during annealing. The number of transitioned samples is charted in Fig. 3(b).

As previously reported [13,21] the characteristic transition time in the random Mg-Y samples is independent of the Y concentration. The same trend can be seen here. Note, that the scatter in our data is significantly larger compared to these references. This is caused by the fact that we only annealed with one velocity initialization per sample. The chemically equilibrated MC Mg-Y samples on the other hand show systematically longer transition times. Moreover, comparing the data shown in Fig. 3(b) we can see that the number of samples where the $\langle \mathbf{c}+\mathbf{a} \rangle$ pyII configuration remained stable is substantially higher in the MC annealed samples compared to the random ones.

These findings clearly show that the solute cloud forming around the dislocation not only reduces the PBT transition but effectively prevents the transition in a number of cases.

To determine the origin of this substantial stabilization we investigated the thermodynamics of the transition in more detail. Fig. 4 shows the energy difference ΔE between the initial pyII dislocation configuration and the basal $\langle \mathbf{c}+\mathbf{a} \rangle$ dislocations after the PBT. The inset schematically shows this energy difference. Note, that we average the energy for $\ln(r/r_0)$ values from 0.35 to 1. The total dislocation energies were calculated as described in Refs. [13,21].

Naturally, we are limited by the subset of samples showing the PBT during our simulations (*cf.* Fig. 3(b)). Nevertheless, a clear trend can be established. While the random Mg-Y samples show a constant energy reduction following the PBT, the MC Mg-Y samples show that this energy difference decreases substantially. The core energy reduction during the PBT is driving force for this transition. Therefore, reducing this energy difference leads to a more stable pyII $\langle \mathbf{c}+\mathbf{a} \rangle$ dislocation. Comparing our findings to Refs. [13,21], we can see that although our smaller number of samples leads to a larger variance in ΔE, the values and trends appear to be quite reasonable.

During the PBT of a solute-decorated dislocation, the dislocation has to move away from the solute cloud, leading to an energetically unfavorable high Y concentration away from the dislocation. This effect gets more pronounced as the Y concentration increases (*cf.* Fig. 1) explaining the trends of ΔE seen above. In the random Mg-Y samples on the other hand, the initial and final atomic environment for the PBT are self similar, therefore the

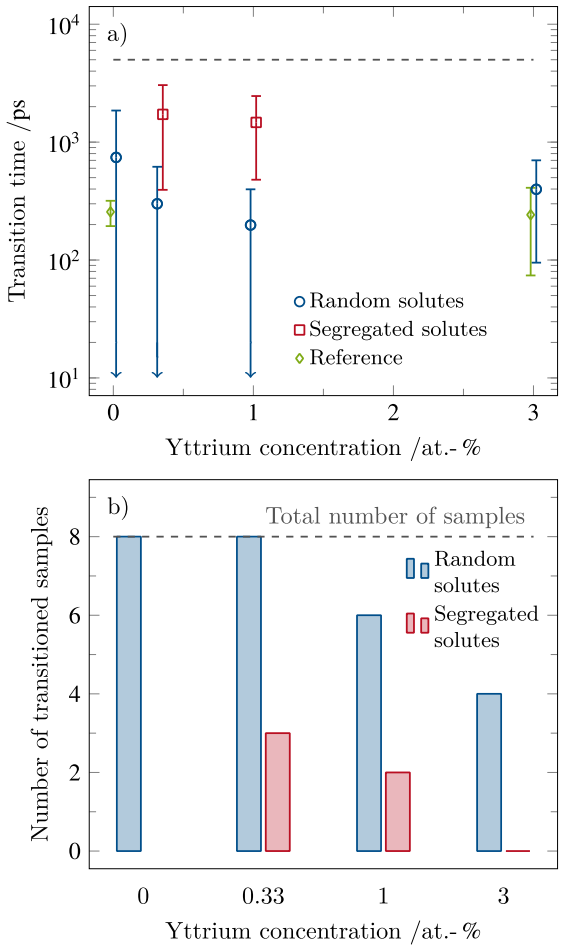

Fig. 3. Mean characteristic transition time from the $\langle \mathbf{c}+\mathbf{a} \rangle$ pyII dislocation to the $\langle \mathbf{c}+\mathbf{a} \rangle$ basal dislocation as function of the Yttrium concentration (a). All samples were annealed for up to 5 ns (indicated by the dashed line). Reference data is taken from Refs. [13,21]. Note that the error bars are distorted due to the logarithmic y-axis and that the x-values are slightly shifted for improved readability. (b) gives the total number of samples that shows the $\langle \mathbf{c}+\mathbf{a} \rangle$ PBT. Only the samples that transitioned were included in the mean transition time given in (a).

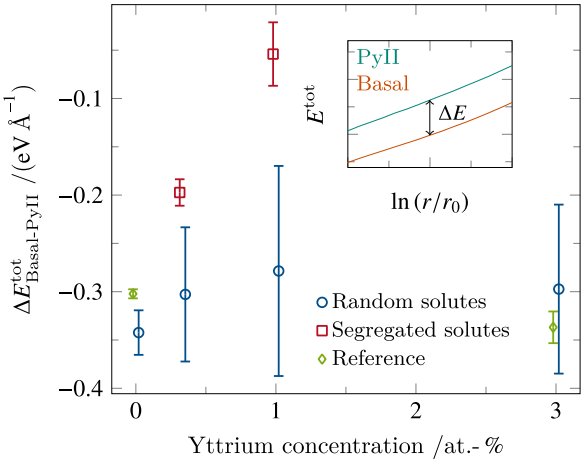

Fig. 4. Difference in the dislocation line energy basal $\langle c+a \rangle$ and the pyramidal II $\langle c+a \rangle$ dislocation configuration in the different samples. Only samples where the structural transition occurred are shown (cf. Fig. 3(b)). The energy difference is averaged over a interval from $\ln(r/r_0) = 0.35$ to 1. Reference data is taken from Wu and Curtin [13,21].

energy difference associated to this transition becomes independent of the Y concentration.

As shown above, the accumulation of Y around the pyII $\langle \mathbf{c}+\mathbf{a} \rangle$ dislocation leads to a strong stabilization against the PBT. This requires diffusional mass transport to the tensile strain side of the dislocation. We compare the characteristic time t^* required for solute cloud formation around the dislocation [27] with the PBT transition time in the random alloy. The case of random alloy serves as the lowest bound for the PBT transition time due to the fact that even partial segregation of solutes in the intermediate steps should increase the transition time. Curtin *et. al.* have introduced the "cross-core" diffusion as the mechanism responsible for solute segregation to dislocations [29]. This mechanism happens at a faster rate than bulk diffusion due to a strong thermodynamic driving force for solutes to migrate from the compressive to the tensile side (or vice versa depending on the solute misfit volume), during periods where dislocations are stopped by other obstacles. The "cross-core" characteristic time t^* for solutes to accumulate in the dislocation core is given by Curtin et al. [29] :

$$t^* \propto [\nu_0 \exp -(\Delta H - \Delta W/2)/k_B T]^{-1} \quad (1)$$

where ΔH is th activation enthalpy, ν_0 is the attempt frequency, k_B is the Boltzmann constant, T is the temperature and ΔW is the average solute-dislocation binding energy difference between tension/compression sides.

Using the experimental activation energy for diffusion of Y in Mg [30] of 1.02 eV and the maximum solute-dislocation binding energy (on one side) specific for the MEAM interatomic potential (W = 563 meV)[23] and a generic attempt frequency of $\nu_0 = 10^{12}$ Hz, we obtain a characteristic time of $t^* = 1.98 \times 10^{-9} s$ at T=700$^\circ K$. This value is comparable to the transition times for PBT in random Mg-Y alloys, at the same temperature, presented in Fig. 3. Therefore, a proper heat treatment prior to deformation can facilitate the segregation of solutes to the pyII $\langle \mathbf{c}+\mathbf{a} \rangle$ dislocations, which will subsequently defer the undesired PBT. Note that in order to compare the characteristic times at all temperatures, the activation energy for the PBT process is required. Obtaining the energy barrier for this transformation requires extensive nudged-elastic-band calculations that are beyond the scope of this paper.

Moreover, segregation of solutes to dislocations can cause pinning by the solute cloud, leading to an increased strength but also brittleness of the alloy. Further analysis is required to compare the cost of pinning the glide of mobile $\langle \mathbf{c}+\mathbf{a} \rangle$ on pyII planes with formation of sessile basal configurations. This is out of scope for this paper.

Nevertheless, this work offers proof of concept for a chemically inhomogeneous Mg-x alloy, where a fast diffusing alloying element x can be used to stabilize the glissle pyII $\langle \mathbf{c}+\mathbf{a} \rangle$ dislocation against transformation to the sessile basal $\langle \mathbf{c}+\mathbf{a} \rangle$ dislocation. Other candidate alloying elements that behave similar to Y in this regard include rare earth elements such as Gd and Ce due to their fast diffusion and strong interaction with dislocation cores caused by their large misfit volumes in Mg. Application of segregation engineering to Mg alloys is particularly important since the bulk solubility of most elements in Mg is rather low. However, strategies to take advantage of segregation at defects can lead to locally high concentration of solutes, thereby changing deformation behavior in ways that smaller amounts of solutes, based on bulk solubility limit, cannot achieve.

We Investigated the effect of Y solute cloud formation around the pyII $\langle \mathbf{c}+\mathbf{a} \rangle$ dislocation in Mg on its stability towards the transition to the basal $\langle \mathbf{c}+\mathbf{a} \rangle$ dislocation.

Using a MC algorithm, we find substantial accumulation of Y in the tensile strain region around the dislocation, accompanied by a depletion in the compressive strain region. Annealing random Mg-Y solid solutions and the samples containing the solute cloud around the dislocation reveals a systematic increase in the pyII to basal dislocation transition time. In the sample with the highest Y concentration, the dislocation reaction could be suppressed entirely. Detailed analysis revealed, that the presence of the Y solute cloud around the initial pyII $\langle \mathbf{c}+\mathbf{a} \rangle$ dislocation reduces the driving force for the dislocation transition and might even lead to themodynamically stable pyII dislocation. In addition, we showed that the characteristic time required for segregation of solutes to dislocations is comparable to the PBT transition time, suggesting the feasibility of solute segregation engineering approaches prior to deformation.

Understanding the effects of the solute cloud on other mechanical properties like ductility and brittleness requires further investigation. Nevertheless, local chemical inhomogeneities can explain the observed experimental stabilization of the pyII $\langle \mathbf{c}+\mathbf{a} \rangle$ dislocation in Mg-x solid solutions and offers a new path to explore in search of ductile Mg for light weight applications.

Declaration of Competing Interest

Authors report no competing interests.

Acknowledgment

The authors would like to acknowledge financial support by the Deutsche Forschungsgemeinschaft (DFG) under grant no. STU 611/2-1 as part of the SPP 2006. MG was supported by the National Science Foundation grant DMR-1709236. Calculations for this research were conducted on the Lichtenberg high performance computer of the TU Darmstadt.

References

[1] M. Neubronner, T. Bodmer, C. Hübner, P.B. Kempa, E. Tsotsas, A. Eschner, G. Kasparek, F. Ochs, H. Müller-Steinhagen, H. Werner, M.H. Spitzner, VDI Heat Atlas, Springer Berlin Heidelberg, 2010, pp. 551–614.
[2] M.K. Kulekci, Int. J. Adv. Manuf. Technol. 39 (2008) 851–865.
[3] H. Friedrich, S. Schumann, J. Mater. Process. Technol. 117 (2001) 276–281.
[4] B.L. Mordike, T. Ebert, Mater. Sci. Eng. A 302 (1) (2001) 37–45.
[5] N.E. Prasad, R.J.H. Wanhill, Volume 1 in Aerospace Materials and Material Technologies, Springer, 2017.
[6] A. Stevenson, JOM 39 (1987) 16–19.
[7] T.M. Pollock, Science 328 (2010) 986–987.
[8] J.-P. Immarigeon, R. Holt, A. Koul, L. Zhao, W. Wallace, J. Beddoes, Mater. Charact. 35 (1995) 41–67.
[9] G. Cole, A. Sherman, Mater. Charact. 35 (1995) 3–9.
[10] A. Heinz, A. Haszler, C. Keidel, S. Moldenhauer, R. Benedictus, W. Miller, Mater. Sci. Eng. A 280 (2000) 102–107.
[11] W. Miller, L. Zhuang, J. Bottema, A. Wittebrood, P. De Smet, A. Haszler, A. Vieregge, Mater. Sci. Eng. A 280 (2000) 37–49.
[12] P.M. Anderson, J.P. Hirth, J. Lothe, Theory of Dislocations, 2017 edition, Cambridge University Press, 2017.
[13] Z. Wu, W.A. Curtin, Nature 526 (2015) 62–67.
[14] S.R. Agnew, J.W. Senn, J.A. Horton, JOM 58 (2006) 62–69.
[15] S. Sandlöbes, S. Zaefferer, I. Schestakow, S. Yi, R. Gonzalez-Martinez, Acta Mater. 59 (2011) 429–439.
[16] S. Sandlöbes, M. Friák, S. Zaefferer, A. Dick, S. Yi, D. Letzig, Z. Pei, L.-F. Zhu, J. Neugebauer, D. Raabe, Acta Mater. 60 (2012) 3011–3021.
[17] S. Sandlöbes, M. Friák, J. Neugebauer, D. Raabe, Mater. Sci. Eng. A 576 (2013) 61–68.
[18] S. Agnew, L. Capolungo, C. Calhoun, Acta Mater. 82 (2015) 255–265.
[19] B. Yin, Z. Wu, W. Curtin, Acta Mater. 136 (2017) 249–261.
[20] Z. Wu, R. Ahmad, B. Yin, S. Sandlöbes, W.A. Curtin, Science 359 (2018) 447–452.
[21] R. Ahmad, Z. Wu, S. Groh, W. Curtin, Scr. Mater. 155 (2018) 114–118.
[22] S. Plimpton, J. Comput. Phys. 117 (1995) 1–19.
[23] R. Ahmad, S. Groh, M. Ghazisaeidi, W.A. Curtin, Model. Simul. Mater. Sci. Eng. 26 (2018) 065010.
[24] P. Hirel, Comput. Phys. Commun. 197 (2015) 212–219.
[25] P.M. Larsen, S. Schmidt, J. Schiøtz, Model. Simul. Mater. Sci. Eng. 24 (2016) 055007.
[26] A. Stukowski, Model. Simul. Mater. Sci. Eng. 18 (2010) 015012.
[27] A.H. Cottrell, B.A. Bilby, Proc. Phys. Soc. A 62 (1949) 49–62.
[28] S.A. Shakhshir, M. Medraj, JPED 27 (2006) 231–244.
[29] W.A. Curtin, D.L. Olmsted, L.G. Hector, Nat. Mater. 5 (2006) 875–880.
[30] S. Das, Y. Kang, T. Ha, J.I. H., Acta Mater. 71 (2014) 164–175.